Thermoosmotic Transport in Nanochannels Grafted with pH-responsive Polyelectrolyte Brushes Modelled Using Augmented Strong Stretching Theory: Online Supplementary Materials

Vishal Sankar Sivasankar, Sai Ankit Etha, Harnoor Singh Sachar, and Siddhartha Das*
Department of Mechanical Engineering, University of Maryland, College Park, MD-20742, USA
(Dated: March 9, 2021)

I. VARIATION OF CONTRIBUTIONS OF INDIVIDUAL IONS TO THE COMPONENTS OF THERMOOSMOTICALLY INDUCED ELECTRIC FIELD

Fig. S1 shows the variation of $\bar{E}_{ion,N,i}$ for $i = \pm, H^+$. We study these variations to explain the corresponding variation of $\bar{E}_{ion,N}$ [shown in Fig. 3(b) in the main paper]. We do not show the contribution of OH^- as its contribution to $\bar{E}_{ion,N}$ is negligible when compared to the contributions from other ions. The variation of $\bar{E}_{ion,N,+}$ with salt concentration is plotted in Fig. S1(a). The variation of $\bar{E}_{ion,N,+}[\propto R_+\exp(-\bar{\psi})]$ primarily depends on the EDL potential ψ for a given temperature gradient dT/dx. It can be seen that the $\bar{E}_{ion,N,+}$ decreases (in magnitude) monotonically with increasing salt concentration. This decrease is due to the decrease in the magnitude of the EDL potential ψ with an increase in c_∞ (as discussed in the main paper). Such a behavior is observed for all cases of brush-grafted nanochannel and brush-less nanochannel. This decrease is much pronounced at intermediate salt concentrations ($c_\infty \sim 10^{-pH_\infty}$) owing to a prominent decrease in the EDL potential at these concentrations. At much lower concentrations ($c_\infty \ll 10^{-pH_\infty}$), the decrease in the magnitude of the EDL potential with salt concentration is weak due to EDL overlap. This leads to a weaker decrease in $\bar{E}_{ion,N,+}$ with an increase in c_∞ for such c_∞ values. Also, at much higher concentrations ($c_\infty \gg 10^{-pH_\infty}$), the EDL potential is much weaker ($|\bar{\psi}| \ll 1$), and hence the $\bar{E}_{ion,N,+}$

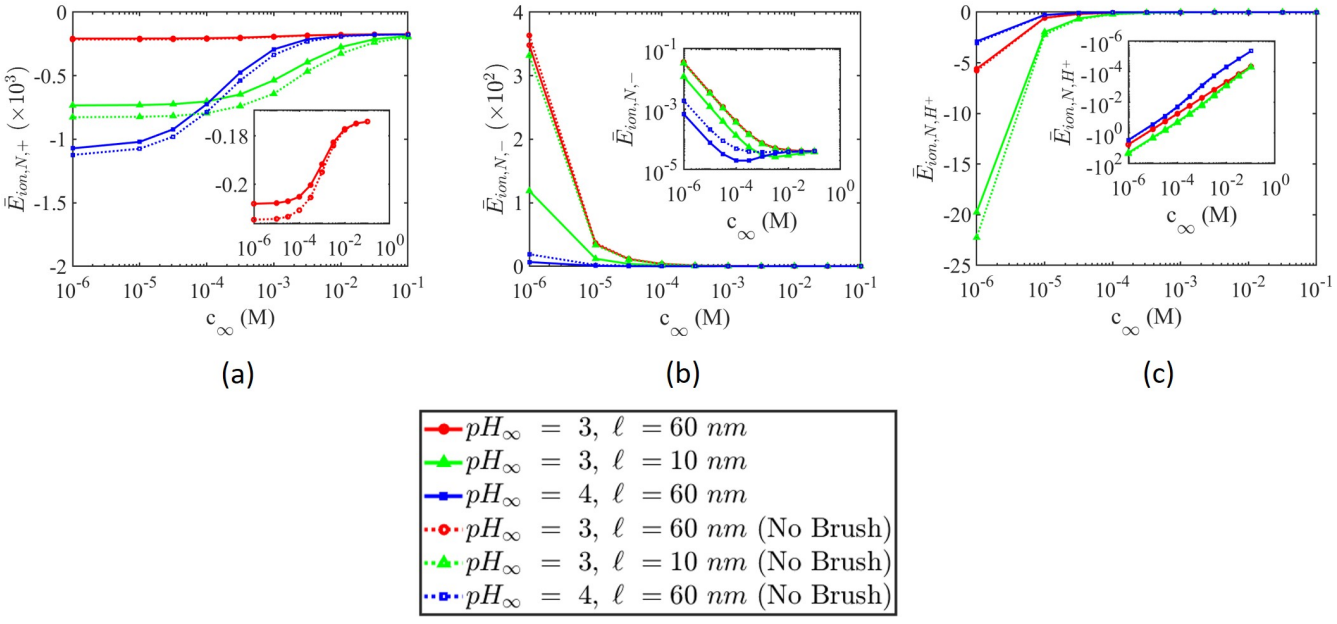

FIG. S1: Variation of (a) $\bar{E}_{ion,N,+}$, (b) $\bar{E}_{ion,N,-}$, and (c) $\bar{E}_{ion,N,H^+}$ [see eq.(30) in the main manuscript for their definitions] with salt concentration (c_∞) in the presence of applied temperature gradient. In the inset of Fig. S1(a), we provide a more magnified view of the $\bar{E}_{ion,N,+}$ for the case of $pH_\infty = 3, \ell = 60\ nm$. In the inset of Figs. S1(b) and S1(c), we show the logarithmic plot of variation of $\bar{E}_{ion,N}$, and $\bar{E}_{diff}$ respectively with salt concentration. All parameters are same as mentioned in Fig. 2 in the main manuscript.

* sidd@umd.edu

approaches a constant value ($\bar{E}_{ion,N,+} \approx -LP_+ \frac{\nabla T}{T} R_+$). For instance, for the case of $pH_\infty = 3,\ \ell = 10\ nm$, we witness a very gradual decrease in the magnitude of $\bar{E}_{ion,N,+}$ in the salt concentration range $10^{-6} - 10^{-4}\ M$. This is followed by a steep decrease in its magnitude in the salt concentration range of $10^{-4} - 10^{-2}\ M$. As we increase the concentration further, we witness $\bar{E}_{ion,N,+}$ gradually approaching a constant value. Similarly, for the case of $pH_\infty = 4,\ \ell = 60\ nm$, we witness a gradual decrease in magnitude of $\bar{E}_{ion,N,+}$ in salt concentration range $10^{-6} - 10^{-5}$. Further, in the salt concentration range $10^{-5} - 10^{-2.5}\ M$, there is a prominent decreases in the magnitude of $\bar{E}_{ion,N,+}$, and at salt concentrations above this the $\bar{E}_{ion,N,+}$ gradually approaches a nearly constant value. In the inset of Fig. S1(a), we show that for the case of $pH_\infty = 3,\ \ell = 60\ nm$ we observe a weak, a significant, and again a weak decrease in the magnitude of $\bar{E}_{ion,N,+}$ in the salt concentration ranges $10^{-6} - 10^{-4}\ M$, $10^{-4} - 10^{-1.5}\ M$, and $10^{-1.5} - 10^{-1}\ M$, respectively.

In Fig. S1(b), we study the variation of $\bar{E}_{ion,N,-}$ with salt concentration for various pH_∞ and ℓ. We witness a decrease in the (positive) magnitude of $\bar{E}_{ion,N,-}$ [$\propto \nabla \bar{n}_{-,\infty} \exp(\bar{\psi}) \propto \frac{n_{-,\infty}}{n_{+,\infty}} \exp(\bar{\psi})$] with increasing salt concentration for all the cases at lower concentrations ($c_\infty \leq 10^{-pH_\infty}$). Since $\bar{n}_{-,\infty} = \frac{n_{-,\infty}}{n_{+,\infty}} = 1 + \frac{1}{\frac{n_\infty}{n_{H^+,\infty}}}$ decreases prominently in this regime of very low concentration ($c_\infty \leq pH_\infty$), we see a rapid decrease in $\bar{E}_{ion,N,-}$. It is to be noted that at these concentrations, the (negative) magnitude of the EDL potential decreases which increases $\exp(\bar{\psi})$ opposing the effect of decrease in $\bar{n}_{-,\infty}$. However, the effect of decreasing magnitude of $\bar{n}_{-,\infty}$ is much dominant in this salt concentration range leading to a net steep decrease in $\bar{E}_{ion,N,-}$. Nevertheless, we see a very small increase of $\bar{E}_{ion,N,-}$ in higher concentration range ($c_\infty \geq pH_\infty$) due to a small decrease in $\bar{\psi}$. As we further increase the salt concentration, $\bar{E}_{ion,N,-}$ reaches a nearly constant value as a result of weak EDL potential $|\bar{\psi}| \ll 1$ and $\bar{n}_{-,\infty} \approx 1 + \bar{n}_{H^+,\infty} \approx 1$ in this region. For example, for the case of $pH_\infty = 3,\ \ell = 10\ nm$, we witness a sharp monotonic decrease in $\bar{E}_{ion,N,-}$ in the salt concentration range $10^{-6} - 10^{-3}\ M$. This is later followed by a slight increase in its magnitude at salt concentration range of $10^{-3} - 10^{-1}\ M$. Similarly, for the case of $pH_\infty = 4,\ \ell = 60\ nm$, we witness a steep decrease in the magnitude of $\bar{E}_{ion,N,-}$ from $c_\infty \sim 10^{-6} - 10^{-4}\ M$. As we increase the salt concentration, we witness a gradual increase in $\bar{E}_{ion,N,-}$ approaching a nearly constant value. For the case of $pH_\infty = 3,\ \ell = 60\ nm$, we witness a monotonic decrease in the magnitude throughout the range of selected salt concentrations. This is because at high salt concentrations the decrease in the EDL potential is too weak to cause any noticeable increase in the magnitude of $\bar{E}_{ion,N,-}$.

Next, we plot the variation of $\bar{E}_{ion,N,H^+}$ [$\propto \nabla \bar{n}_{H^+,\infty} \exp(-\bar{\psi}) \propto \frac{n_{H^+,\infty}}{n_{+,\infty}} \exp(-\bar{\psi})$] with salt concentration in Fig.S1(c). $\bar{E}_{ion,N,H^+}$ decreases with increasing salt concentration. The reduced bulk number density of H^+ ions ($\bar{n}_{H^+,\infty} = \frac{n_{H^+,\infty}}{n_{+,\infty}}$) and the (magnitude of the negative) EDL potential decreases sharply with c_∞ at low concentration ($c_\infty \leq pH_\infty$) leading to a steep decrease in the magnitude of $\bar{E}_{ion,N,H^+}$. At higher salt concentration ($c_\infty \gg pH_\infty$), as the magnitude of EDL potential $|\bar{\psi}| \ll 1$, $\bar{E}_{ion,N,H^+}$ decreases in magnitude with increasing salt concentration [see the inset of Fig. S1(c)]. This is due to the decrease in $\bar{n}_{H^+,\infty}$ with increase of n_∞ with increasing salt concentration. This is seen clearly for all the three brush grafted cases and the corresponding brushless cases. In fact, like $\bar{E}_{ion,N,H^+}$, we observe very similar trends for the corresponding brushless nanochannels for $\bar{E}_{ion,N,+}$ [see Fig.S1(a)] and $\bar{E}_{ion,N,-}$ [see Fig.S1(b)].

Fig. S2 shows the variation of $\bar{E}_{t,N,i}$ with salt concentration for ions $i = \pm, H^+$. Here, we do not show the contribution of the OH^- ion to the $\bar{E}_{t,N}$ as it is negligible in comparison to the contribution of other ions. First, we study the variation of $\bar{E}_{t,N,+}$, which is plotted in Fig. S2(a). We witness a monotonic increase in $\bar{E}_{t,N,+}$ with increasing salt concentration (c_∞). Here the term "increase" implies a decrease in magnitude when $\bar{E}_{t,N,+}$ is negative, and implies an increase in magnitude when $\bar{E}_{t,N,+}$ is positive. The variation of $\bar{E}_{t,N,+}$ depends on the interplay of two opposing factors: $(\bar{Q}_+ + \bar{\psi})$ which increases with increasing salt concentration, and $\exp(-\bar{\psi})$ which decreases with salt concentration (as $\bar{\psi}$ decreases in magnitude and is negative). The former is instrumental in determining the sign of the quantity given that the latter is always positive. Here, we witness a gradual increase in $\bar{E}_{t,N,+}$ at very low concentration ($c_\infty \ll 10^{-pH_\infty}$). This is followed by a steep increase in the value of $\bar{E}_{t,N,+}$ at intermediate concentrations ($c_\infty \sim 10^{-pH_\infty}$). Eventually $\bar{E}_{t,N,+}$ approaches a constant value at higher concentration ($c_\infty \gg 10^{-pH_\infty}$). This is because in the lower concentration region ($c_\infty \ll 10^{-pH_\infty}$), the EDL thickness is much larger resulting in a overlap of EDL which results in nearly constant EDL potential for different c_∞. At intermediate concentrations, $\bar{E}_{t,N.+}$ varies significantly owing to a steep decrease in the EDL potential in this concentration range (see the discussion on EDL potential in the main paper). However, for larger concentrations ($c_\infty \gg 10^{-pH_\infty}$) where $\bar{\psi} \ll 1$ and there is no significant variation of $\bar{\psi}$, there is a very gradual increase of $\bar{E}_{t,N,+}$ approaching a nearly constant value. For instance, for the case of $pH_\infty = 3, \ell = 10\ nm$, we witness a nearly constant $\bar{E}_{t,N,+}$ in the concentration range $10^{-6} - 10^{-4}\ M$ followed by a steep increase of $\bar{E}_{t,N.+}$ from $c_\infty \sim 10^{-4} - 10^{-2}\ M$ and a nearly constant $\bar{E}_{t,N,+}$ in $c_\infty \sim 10^{-2} - 10^{-1}\ M$. Similarly, for the case of $pH_\infty = 4, \ell = 60\ nm$, we observe a very gradual increase, followed by a steep increase, and

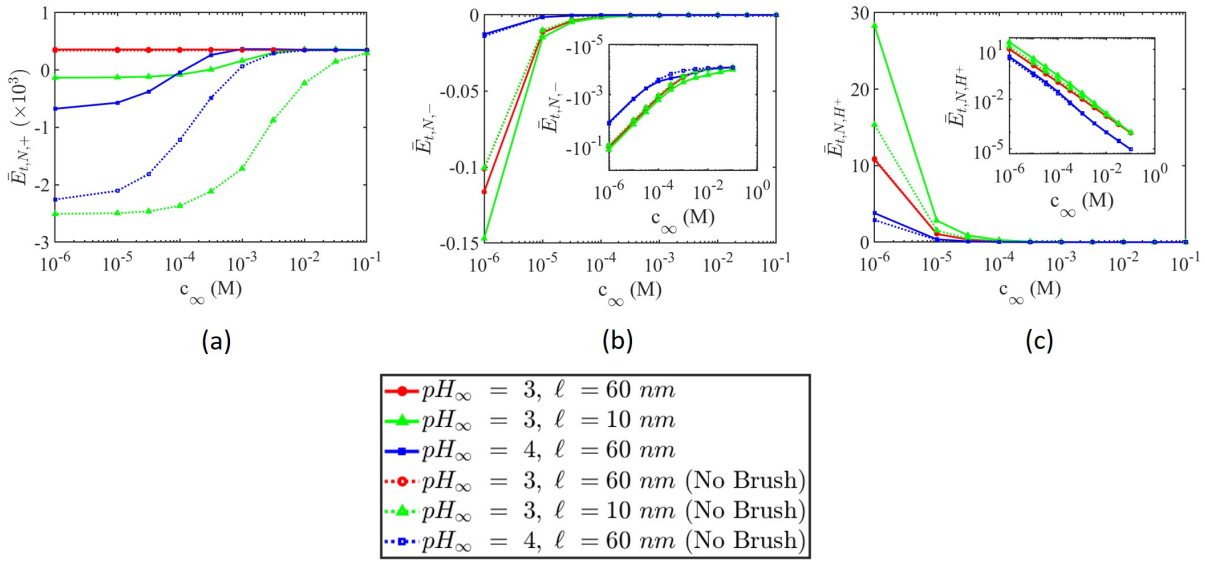

FIG. S2: Variation of (a) $\bar{E}_{t,N,+}$, (b) $\bar{E}_{t,N,-}$, and (c) $\bar{E}_{t,N,H^+}$ [see eq.(31) in the main manuscript for their definition] with salt concentration (c_∞) in the presence of applied temperature gradient. In the inset of Figs. S2(b) and S2(c), we provide the logarithmic plot of variation of $\bar{E}_{t,N,-}$ and $\bar{E}_{t,N,H^+}$ respectively with salt concentration. All parameters are same as mentioned in Fig. 2 in the main manuscript.

then attainment of a nearly constant value of $\bar{E}_{t,N,+}$ for concentration ranges of $10^{-6}-10^{-5}\ M$, $10^{-5}-10^{-2.5}\ M$, and $10^{-2.5}-10^{-1}\ M$ respectively. It is to be observed that for the case of $pH_\infty = 3, \ell = 60\ nm$, the change in $\bar{E}_{t,N,+}$ is very small with respect to c_∞ owing to weak EDL potential. $\bar{E}_{t,N,+}$ is always positive for this case as $\bar{Q}_+ + \bar{\psi}$ is always positive for this case given the weak EDL potential (i.e. $\bar{Q}_+ > |\bar{\psi}|$). However, for the cases of $pH_\infty = 3, \ell = 10\ nm$ and $pH_\infty = 4, \ell = 60\ nm$, we witness a negative $\bar{E}_{t,N,+}$ at lower salt concentrations, and a positive $\bar{E}_{t,N,+}$ at much higher salt concentrations. This is because with increasing salt conentration, $\bar{Q}_+ + \bar{\psi}$ becomes less negative as $\bar{\psi}$ becomes less negative (as it decreases in magnitude) and $\bar{Q}_+ + \bar{\psi}$ becomes positive at higher concentrations where $\bar{Q}_+ > |\bar{\psi}|$ is satisfied. The difference in $\bar{E}_{t,N,+}$ between the brush-grafted and brush-free cases is due to the difference in the EDL potential distribution. For the case of brush-less nanochannels, the condition of $\bar{Q}_+ > |\bar{\psi}|$ is satisfied at much higher concentration when compared to brush-grafted case, which results in the $\bar{E}_{t,N,+}$ becoming positive at a much higher concentration than the brush-grafted counterparts. This large variation in $\bar{E}_{t,N,+}$ [as witnessed in Fig. S2(a)] is due to much localized and stronger EDL of the brushless cases in comparison to the corresponding brush-grafted cases.

We next study the variation of $\bar{E}_{t,N,-}$ with salt concentration in Fig. S2(b). The variation of $\bar{E}_{t,N,-}$ ($\propto \bar{n}_{-,\infty}(\bar{Q}_- - \bar{\psi})\exp(\bar{\psi})$) depends on the EDL potential $\bar{\psi}$ and the reduced bulk number density of -ve ions. It is clear from the plot that $\bar{E}_{t,N,-}$ shows a steep decrease in magnitude with c_∞ for smaller c_∞ values ($c_\infty \ll 10^{-pH_\infty}$), followed by gradual decrease approaching a constant value at concentrations $c_\infty > 10^{-pH_\infty}$. For smaller c_∞ ($c_\infty < 10^{-pH_\infty}$), with increasing salt concentration $\bar{n}_{-,\infty}(\approx 1 + \frac{n_{H^+,\infty}}{n_\infty})$ decreases which is opposed by an increase of $\exp(\bar{\psi})$ (as $\bar{\psi}$ is -ve and it decreases in magnitude). This interplay results in a steep decrease in the magnitude of $\bar{E}_{t,N.-}$ following the dominant effect of the variation of $\bar{n}_{-,\infty}$. However, at higher concentration ($c_\infty > 10^{-pH_\infty}$), the reduced bulk number density of -ve ions ($n_{-,\infty} \approx 1 + \bar{n}_{H^+,\infty} \approx 1$) becomes nearly constant, and the EDL potential $\bar{\psi}$ becomes insignificant ($|\bar{\psi} \ll 1|$) resulting in a nearly constant $\bar{E}_{t,N,-}$. For instance, we see a steep decrease in the magnitude of $\bar{E}_{t,N.-}$ for $c_\infty \sim 10^{-6}-10^{-3}\ M$ followed by a gradual decrease to a constant value for in the concentration range of $10^{-3}-10^{-1}\ M$ for both the cases of $pH_\infty = 3, \ell = 60\ nm$ and $pH_\infty = 3, \ell = 10\ nm$. Similarly, for the case of $pH_\infty = 4, \ell = 60\ nm$, we observe a steep decrease in magnitude of $\bar{E}_{t,N,-}$ from c_∞ of $10^{-6}-10^{-4}\ M$ followed by a small decrease in its magnitude at the salt concentration range $10^{-4}-10^{-1}\ M$.

In Figure S2(c), we plot the variation of $\bar{E}_{t,N,H^+}$ with salt concentration. It is to be noted that the $\bar{E}_{t,N,H^+}$ always remains positive given that $\bar{Q}_{H^+} \gg |\bar{\psi}|$ for all combinations of parameters reported. At lower concentrations ($c_\infty < 10^{-pH_\infty}$), we see prominent decrease in $\bar{E}_{t,N,H^+}$ ($\propto \frac{n_{H^+,\infty}}{n_\infty}(\bar{Q}_{H^+} + \bar{\psi})\exp(-\bar{\psi})$). In this region, both the reduced number density of H^+ ions $\bar{n}_{H^+,\infty}$ and $|\bar{\psi}|$ decreases resulting in such a steep monotonic decrease in magnitude of $\bar{E}_{t,N,H^+}$. However, at higher concentration region ($c_\infty \gg 10^{-pH_\infty}$), $\bar{E}_{t,N,H^+}$ decreases with increasing salt

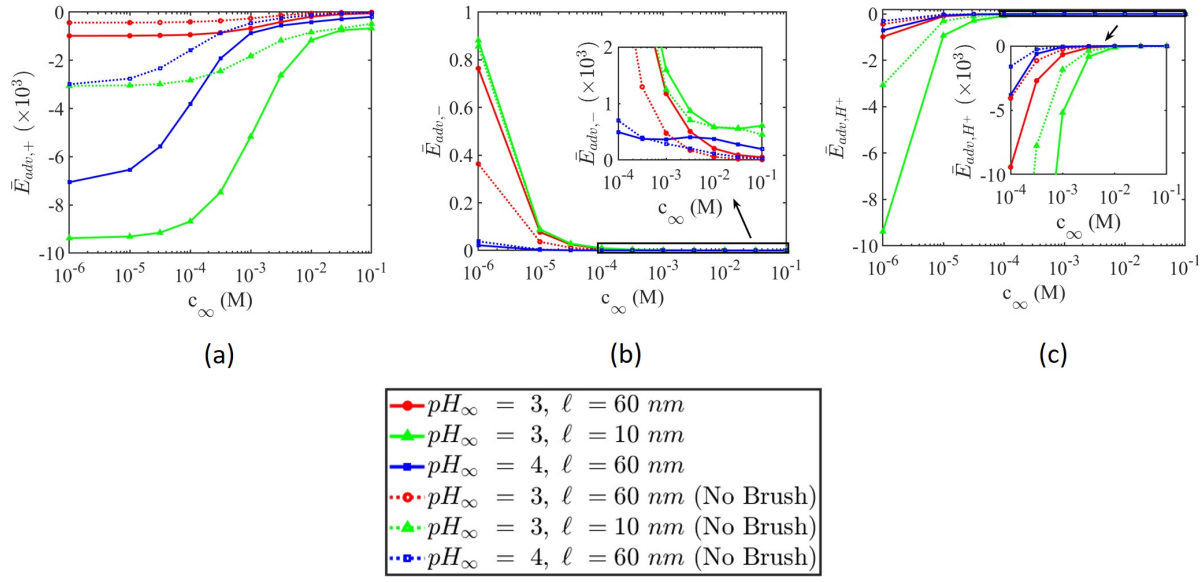

FIG. S3: Variation of (a) $\bar{E}_{adv,+}$, (b) $\bar{E}_{adv,-}$, and (c) $\bar{E}_{adv,H^+}$ [see eq.(32) in the main manuscript for their definitions] with salt concentration (c_∞) in the presence of applied temperature gradient. In the inset of Figs. S3(b) and S3(c), we provide more magnified views of the respective variations of $\bar{E}_{adv,-}$ and $\bar{E}_{adv,H^+}$ at higher salt concentrations. The contribution of OH^- ions is not shown as its contribution is negligible in comparison to other ions contribution. All parameters are same as mentioned in Fig. 2 in the main manuscript

concentration as n_∞ increases and given that EDL potential is weak ($\exp(-\bar{\psi}) \approx 1 - \bar{\psi} \approx 1$). For example, for all the cases we witness a steeper decrease in the magnitude of $\bar{E}_{t,N.+}$ in the concentration range $10^{-6} - 10^{-pH_\infty}$ M. This is followed by a decrease in its magnitude with respect to c_∞ from $10^{-pH_\infty} - 10^{-1}$ M [see the inset of Fig.S2(c)]. Finally, we shall like to point out that the variations of $\bar{E}_{t,N,-}$ and $\bar{E}_{t,N,H^+}$ for the brush-free cases are much similar to that of corresponding brush grafted cases.

In Fig. S3(a), we study $\bar{E}_{adv,+} - vs - c_\infty$ for various pH_∞, and ℓ. The variation of $\bar{E}_{adv,+}$ with c_∞ depends on the dimensionless TOS velocity $\bar{u}$, and EDL potential $\bar{\psi}$ [$\bar{E}_{adv,+} \propto \bar{u}\exp(-\bar{\psi})$]. With increasing salt concentration both EDL potential ($\bar{\psi}$) (see Fig. 4 in the main paper) and dimensionless TOS velocity ($\bar{u}$) decreases monotonically (see Fig. 8 in the main paper). It is interesting to note that the $\bar{E}_{adv,+}$ depends mainly on $\bar{u}$ at higher concentrations ($c_\infty > 10^{-pH_\infty}$) as EDL potential becomes significantly small $|\bar{\psi}| \ll 1$. For instance, it can be noted that for the brush-grafted nanochannel for the case of $pH_\infty = 3, \ell = 10$ nm, we see a monotonic decrease in the magnitude of $\bar{E}_{adv,+}$ at lower concentrations ($c_\infty \sim 10^{-6} - 10^{-3}$ M) owing to decrease in both $\bar{\psi}$ and $\bar{u}$. At higher concentration, in the concentration range $c_\infty \sim 10^{-3} - 10^{-1.5}$ M we see a monotonic decrease in the magnitude of $\bar{E}_{adv,+}$ due to similar change in TOS velocity $\bar{u}$ in this range. As we further increase the salt concentration, we see nearly constant magnitude of $\bar{E}_{adv,+}$ in the concentration range ($c_\infty \sim 10^{-1.5} - 10^{-1}$ M) due to corresponding lack of variation in velocity. Similarly, for the case of $pH_\infty = 4, \ell = 60$ nm, we observe a monotonic decrease in magnitude of $\bar{E}_{adv,+}$ due to decrease in EDL potential and velocity in the salt concentration range of $10^{-6} - 10^{-4}$ M. It could be seen that there is a monotonic decrease in the magnitude of $\bar{E}_{adv.+}$ from $c_\infty \sim 10^{-4} - 10^{-3}$ M reflecting the similar decrease in the magnitude of TOS velocity, followed by an nearly constant value (very slight decrease in magnitude because of decrease in $\exp(-\bar{\psi})$) in the range of $10^{-3} - 10^{-2}$ M due to nearly constant TOS velocity $\bar{u}$. This is followed by a slight decrease in the magnitude of $\bar{E}_{adv,+}$ as the TOS velocity decreases in this range. Likewise, for the case of $pH_\infty = 3, \ell = 60$ nm, we notice a monotonic decrease in the magnitude of $\bar{E}_{adv,+}$ for the concentration range of $10^{-6} - 10^{-3}$ M due to a decrease in magnitude of EDL potential and TOS velocity. The magnitude of $\bar{E}_{adv,+}$ decreases as we move further in the range of $10^{-3} - 10^{-1}$ M following the variation of TOS velocity in this same region. The variation of the $\bar{E}_{adv.+}$ can be explained similarly for brushless nanochannels. For example, for the brushless case of $pH_\infty = 3, \ell = 10$ nm, we see a monotonic decrease in magnitude of $\bar{E}_{adv,+}$ in accordance with decrease of $|\bar{\psi}|$ and $\bar{u}$ at lower concentrations till ($c_\infty \sim 10^{-3}$ M). This is followed by a decrease in magnitude of $\bar{E}_{adv,+}$ from $c_\infty \sim 10^{-3} - 10^{-1}$ M as a result of decrease in magnitude of $\bar{u}$ in the same concentration range. For the brushless case of $pH_\infty = 4, \ell = 60$ nm, we notice decrease in the magnitude of $\bar{E}_{adv,+}$ at lower concentrations

($c_\infty < 10^{-4}$) due to decrease in magnitude of $\bar{\psi}$ and $\bar{u}$. As for the higher concentrations, we witness a decrease in $|\bar{E}_{adv,+}|$ for concentrations $c_\infty \sim 10^{-4} - 10^{-1}\ M$ owing to decrease in $\bar{u}$. Similarly, the monotonic variation of the $|\bar{E}_{adv,+}|$ for the brushless nanochannel for $pH_\infty = 3, \ell = 60\ nm$ is due to the variation of $\bar{\psi}$ and $\bar{u}$ in the lower concentration and TOS velocity $\bar{u}$ in the higher concentration.

Subsequently, we analyze the variation of $\bar{E}_{adv,-}$ with salt concentration (c_∞) [see Fig.S3(b)]. At lower concentrations ($c_\infty < 10^{-pH_\infty}$), $\bar{E}_{adv,-} \propto \frac{n_{-,\infty}}{n_\infty} \propto 1 + \frac{n_{H^+,\infty}}{n_\infty}$, which explains the steep decrease in this range due to sharp decrease in $\bar{n}_{-,\infty}$ with increasing concentration. This effect is however opposed by the increase in $\exp(\bar{\psi})$ as $|\bar{\psi}|$ decreases with increasing concentration due to increased screening of EDL by mobile ions. However, the interplay of these two effects results in a net effect of decrease in the magnitude of $\bar{E}_{adv,-}$. At higher concentrations ($c_\infty > 10^{-pH_\infty}$), the TOS velocity has a significant impact on the variation of $\bar{E}_{adv,-}$ with c_∞ as the EDL becomes much weaker ($|\bar{\psi}| \ll 1$) and the reduced bulk number density of -ve ions becomes nearly constant ($\bar{n}_{-,\infty} \approx 1 + \bar{n}_{H^+,\infty} \approx 1$). For the case of $pH_\infty = 3, \ell = 60\ nm$, we see a monotonic decrease in the lower concentration range ($10^{-6} - 10^{-3}\ M$) because of the decrease in $\bar{n}_{-,\infty}$, and as we move further we see a monotonic decrease in the magnitude of $\bar{E}_{adv,-}$ in the concentration range of $10^{-3} - 10^{-1}\ M$ corresponding to similar decrease in $\bar{u}$. For the case of $pH_\infty = 3, \ell = 10\ nm$, at lower concentration range of $10^{-6} - 10^{-3}\ M$ we witness a monotonic decrease in magnitude of $\bar{E}_{adv,-}$corresponding to decrease in $\bar{n}_{-,\infty}$. As we move from $10^{-3} - 10^{-1.5}\ M$ we witness reduction of the magnitude of $\bar{E}_{adv,-}$ corresponding to the variation of $\bar{u}$ in this concentration range. This is followed by a slight increase in magnitude of $\bar{E}_{adv,-}$ which reflects a similar increase in TOS velocity from $c_\infty \sim 10^{-1.5} - 10^{-1}\ M$. For the case of $pH_\infty = 4, \ell = 60\ nm$, we observe decrease in magnitude reflecting the decrease in $\bar{n}_{-,\infty}$. At higher concentrations: we witness a increase in the magnitude of $\bar{E}_{adv.-}$ in the range of $c_\infty \sim 10^{-4} - 10^{-3}\ M$ due to the net effect of interplay between the decrease in the magnitude of TOS velocity and the increase in $\exp(\bar{\psi})$. This is followed by a decrease in the magnitude of $\bar{E}_{adv,-}$ as the TOS velocity decreases in this region. Similarly, for the brushless cases as well, it can be seen that the variation of TOS velocity is manifested as the variation of $\bar{E}_{adv,-}$ at large salt concentrations. And at lower salt concentrations, we witness a monotonic decrease similar to the corresponding brush-grafted cases due to the sharp decrease in $\bar{n}_{-,\infty}$. It should be noted that $|\bar{E}_{adv,-}|_{(Brush)} < |\bar{E}_{adv,-}|_{(NoBrush)}$ because of the enhancement of the TOS velocity in the presence of PE brush as explained before.

In Fig. S3(c) we plot the variation of $\bar{E}_{adv,H^+}$ with salt concentration (c_∞). Here, the magnitude of $\bar{E}_{adv,^+} \propto \bar{n}_{H^+,\infty}\bar{u} \propto \frac{n_{H^+,\infty}}{n_\infty}\bar{u}$. So, for given value of pH, an increase in salt concentration results in decrease of $\bar{n}_{H+,\infty}$ leading to a decrease in magnitude of $\bar{E}_{adv,H^+}$. At lower salt concentrations ($c_\infty \sim 10^{-6} - 10^{-pH_\infty}\ M$), this decrease is further supplemented by the decrease in $|\bar{\psi}|$ and TOS velocity, leading to a sharp decrease in the magnitude of $\bar{E}_{adv,H^+}$ as seen in Fig.S3(c). However, at higher concentrations ($c_\infty \gg 10^{-pH_\infty}$), it can be seen that $\bar{n}_{H^+,\infty} \ll 1$ which overwhelms the change due to TOS velocity change resulting in a very small monotonic reduction of $\bar{E}_{adv,H^+}$. This can be seen for all the different cases reported. The brushless cases have a much lower magnitude of $\bar{E}_{adv,H^+}$ as a result of lower magnitude of TOS velocity.